

Carrier-induced ferromagnetism in Ge(Mn,Fe) magnetic semiconductor thin-film structures

R. R. Gareev^{a)}

*Institute of Solid State Research (IFF), Research Centre Jülich, 52425 Jülich, Germany
and Institute of Experimental and Applied Physics, University of Regensburg, 93040 Regensburg, Germany*

Yu. V. Bugoslavsky

Blackett Laboratory, Imperial College, Prince Consort Road, London SW7 2BZ, United Kingdom

R. Schreiber and A. Paul

Institute of Solid State Research (IFF), Research Centre Jülich, 52425 Jülich, Germany

M. Sperl and M. Döppe

Institute of Experimental and Applied Physics, University of Regensburg, 93040 Regensburg, Germany

(Received 21 October 2005; accepted 19 April 2006; published online 31 May 2006)

We report on the carrier-induced ferromagnetism in Ge(Mn,Fe) magnetic semiconductor insulating-type thin-film structures prepared using sequential deposition at $T_g=520$ K with subsequent annealing at T_g . In the resulting films Mn and Fe are diffused in the Ge matrix without compromising the epitaxial structure. The anomalous Hall effect serves as a manifestation of the carrier-induced magnetism, with p -type conductivity and the Curie temperature $T_C=209$ K. The additional doping with Fe stabilizes epitaxial growth and carrier-mediated magnetism at levels of magnetic doping exceeding 10%. We conclude that indirect ferromagnetic exchange is mediated by localized holes with concentration $n \sim 10^{20} \text{ cm}^{-3}$ and mobility $\mu \sim 10 \text{ cm}^2/(\text{V s})$. © 2006 American Institute of Physics. [DOI: 10.1063/1.2208552]

Recently, nonmetallic diluted magnetic semiconductors (DMSs) based on group IV semiconductors (SC) attracted special attention due to their reliability for a straightforward integration into Si-based electronics, relatively high Curie temperature T_C , and specific magnetic and transport properties compared to metallic GaMnAs DMS.^{1–7} The experiments with Ge-based single crystalline Ge(Mn),¹ as well as epitaxial Ge(Fe) (Ref. 2) and Ge(Co,Mn) (Ref. 3) inhomogeneous thin-film structures, demonstrated magnetic ordering close to room temperature. Moreover, the crystalline Si (Mn) films showed ferromagnetic (FM) ordering with T_C even higher than 400 K.⁴ For insulating MnGe films the carrier-induced ferromagnetism (CIFM) with two magnetic phase transitions has been established and related to localization effects with formation and percolation of bound magnetic polarons (BMPs).^{7,8}

Here we report on the CIFM in another DMS compound, an alloy of Ge, Fe, and Mn with high concentration of magnetic dopants, which shows the Curie temperature T_C higher than 200 K. We use the anomalous Hall effect (AHE) as a test probe⁹ to identify a DMS phase. We prove that magnetism below T_C originates from the genuine DMS rather than from ferromagnetic precipitates. We show that codoping with Fe and Mn results in increased T_C and epitaxial growth for total concentrations of dopants exceeding 10%.

We use the protocol of multilayer growth consisting of repeating Ge/Mn/Fe trilayer blocks as described elsewhere.⁶ The nominal thicknesses of Mn and Fe layers were 4 and 2 Å, respectively, so that it was expected that these elements would effectively incorporate into the germanium matrix. We note that we keep the ratio of Mn and Fe constant while

varying the thickness of the Ge spacing layers.

The films were grown on insulating GaAs (001) substrates after a preliminary desorption of a native oxide by annealing at 880 K. The oxygen content and composition of the material were controlled *in situ* using Auger electron spectroscopy. All three elements (Ge, Fe, and Mn) were deposited by molecular beam epitaxy at low deposition rates (0.1 Å/s) and at a fixed substrate temperature $T_g=520$ K. The atomic fluxes were controlled using calibrated quartz crystal monitors. Afterwards, *in situ* annealing was performed at T_g for approximately 16 h.

Resistivity ρ_{xx} and Hall resistivity ρ_{xy} were measured on square shaped unpatterned samples using the van der Pauw method and confirmed for optically patterned samples with the current path along GaAs [110] direction. The well-defined current path enabled to estimate that the anisotropic magnetoresistance is negligible for all studied samples. Magnetization measurements were performed using superconducting quantum interference device (SQUID) magnetometer (Quantum Design) and vibrating sample magnetometer (VSM) (Oxford Instruments).

The periodic layered structure was identified from the low-angle x-ray diffraction data for samples with progressively thinner Ge layers (Fig. 1). For the sample with 80 Å thick Ge (Ge80), sharp diffraction peaks from interfaces are present, whereas the peak amplitude becomes significantly lower and separation of peaks is increased for Ge60. For Ge45 the signal from interfaces is no longer detectable. This confirms that the constituent elements are intermixed without any detectable sublayers remaining. Compared to previous experiments,⁶ we used thinner germanium layers and operated at lower annealing temperatures, thus combining more uniform mixing of elements with reduced precipitation. The in-plane crystalline structure is monitored by the low-energy

^{a)} Author to whom correspondence should be addressed; electronic mail: gareev.rashid@physik.uni-regensburg.de

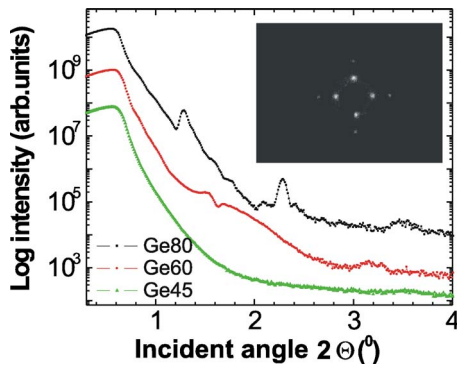


FIG. 1. (Color online) The low-angle x-ray diffraction data for Ge80, Ge60, and Ge45 samples corresponding to the multilayered stack of base Ge(x)/Fe(2 Å)/Mn(4 Å) trilayers with x of 80, 60, and 45 Å; nominal Ge:Mn:Fe compositions of 88:8:4, 84:10.5:5.5, and 80:13:7; and total thicknesses of 172, 136, and 128 nm, respectively. The inset demonstrates the LEED pattern of annealed Ge45 taken at the energy of electrons $E=55$ eV.

electron diffraction (LEED). The LEED pattern (see inset in Fig. 1) confirms formation of epitaxial Ge(Mn,Fe) films on GaAs(001) with the in-plane lattice constant a close to epitaxial Ge ($a \sim 5.6$ Å). We found that the annealing step improves the sharpness of the LEED pattern.

From the analysis of the relative line intensities in Auger spectra for Ge, Mn, and Fe, we have determined the composition of Ge45 sample as $\text{Ge}_{81}\text{Mn}_{13}\text{Fe}_6$, which is in a good agreement with the calculations based on the atomic contents. The LEED and Auger data give a strong indication of incorporation of Mn and Fe dopants in Ge host lattice in spite of high level of codoping.

The spontaneous magnetization data (Fig. 2) revealed presence of ferromagnetic phase with $T_C^{**} = 310 \pm 10$ K, which we relate to residual Mn_5Ge_3 precipitates¹⁰ not detectable by high-angle x-ray diffraction. Note that from our magnetic and x-ray data, we could not identify additional Fe–Mn or ternary Ge–Fe–Mn cluster phases, which possibly formed in our structures.

From the inflection points in the dependence of spontaneous magnetization versus temperature $M(T)$, where $dM/dT(T)$ shows extrema, we found out magnetic phase transition with $T_C = 205 \pm 5$ K (Fig. 2) for Ge60 and Ge45 samples, in contrast to Ge80. Moreover, we managed to resolve additional magnetic phase transition for Ge45 with $T_C^* = 120 \pm 5$ K. Below we demonstrate that magnetic phase

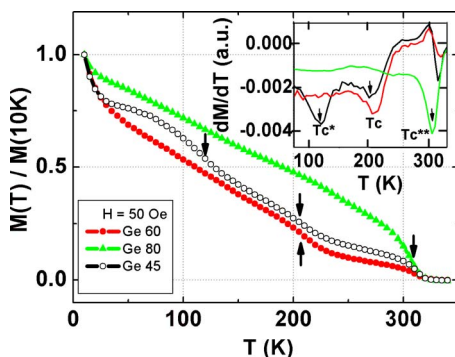


FIG. 2. (Color online) The normalized spontaneous magnetization vs temperature T (SQUID data) for Ge80 (triangles), Ge60 (closed circles), and Ge45 (open circles) samples. Magnetic field $H=50$ Oe is applied along GaAs [110]. The inset shows corresponding dependencies of dM/dT vs temperature T . Arrows indicate temperatures of magnetic phase transitions.

with critical temperature $T_C \sim 205$ K shows C1FM and can be related to DMS phase.

The sample with strongest C1FM, Ge45 (see below), showed the highest value of saturation magnetization $M_{\text{sat}}(10 \text{ K}) \sim 40 \text{ emu/cm}^3$, which was determined from magnetization curves taken by SQUID at $T=10$ K for magnetic fields up to $H=20$ kOe. In contrast, for Ge80 with $M_{\text{sat}}(10 \text{ K}) \sim 12 \text{ emu/cm}^3$, the C1FM was not observed and, thus, the cluster phase is dominant. Then, assuming formation of similar cluster phases for Ge45 and Ge80, we obtained that for Ge45 the DMS phase prevails with the relative impact of clusters to magnetization near 30%.

From magnetization curves for H perpendicular to the film plane and H parallel to the film plane (VSM data), we found the similar values of saturation magnetization M_{sat} , thus confirming formation of a three-dimensional DMS phase. The samples are isotropic in the parallel geometry.

The samples demonstrate continuous decrease of the temperature coefficient of resistivity with decrease of thickness of Ge layers. All studied samples show moderate insulating-type $\rho_{xx}(T)$ dependence without defined anomalies. In particular, for Ge45 starting from $\rho_{xx}(10 \text{ K}) = 8 \times 10^{-5} \Omega \text{ m}$ at $T=10$ K, the total change of resistivity was not exceeding 70%. The magnetoresistance of all studied samples is small and does not exceed 0.5%.

The Hall resistivity ρ_{xy} consists of the normal and the anomalous parts:

$$\rho_{xy} = R_H B + R_A M.$$

To demonstrate the anomalous contribution, we compared the magnetization and Hall data. At $T=10$ K ρ_{xy} for Ge45 exhibits hysteretic behavior, closely matching that of the magnetization. However, already at 20 K the coercivity in the AHE becomes significantly weaker than in the magnetization [Fig. 3(a)]. From the slope of the high-field part of the Hall data, we determined the normal Hall coefficient R_H . The sign of R_H corresponds to holes as majority carriers for all the samples studied. The coexistence of a DMS phase with magnetic precipitates makes the saturation magnetization M_{sat} an imprecise measure of the DMS material. It was therefore more reliable to use the value of ρ_{xy} in the analysis of the AHE rather than the derived value of R_A . We quantified the AHE using the value of the saturation anomalous Hall resistivity $\rho_{xy \text{ sat}}$, as shown in Fig. 3(a).

Taking into account that the DMS phase for Ge45 prevails, we calculated the nominal concentration of holes n and their mobility μ . For Ge45 with strongest C1FM, we found the small increase of n and μ with temperature not exceeding 30% in the temperature range from 10 to 300 K, which serves as a clear indication of strong localization of holes for Ge45 with $\mu = 10 \text{ cm}^2/(\text{V s})$ and $n = 7 \times 10^{19} \text{ cm}^{-3}$ at $T=10$ K.

In Fig. 3(b) we present the temperature dependence of $\rho_{xy \text{ sat}}$ for the Ge45 sample. The inset in Fig. 3(b) reveals clearly the kink at $T_C = 209$ K in a good accordance with the SQUID data, thus confirming formation of the DMS phase. The small part of AHE, which is not exceeding 3% compared to $\rho_{xy \text{ sat}}$ at $T=4.2$ K, still persists even at room temperature. We note that in Ge80 the AHE is negligible and in Ge60 $\rho_{xy \text{ sat}}$ ($T=10$ K) is nearly one order of magnitude smaller compared to that of Ge45. However, the T_C 's of the AHE for Ge45 and Ge60 closely coincide. We relate this result to the

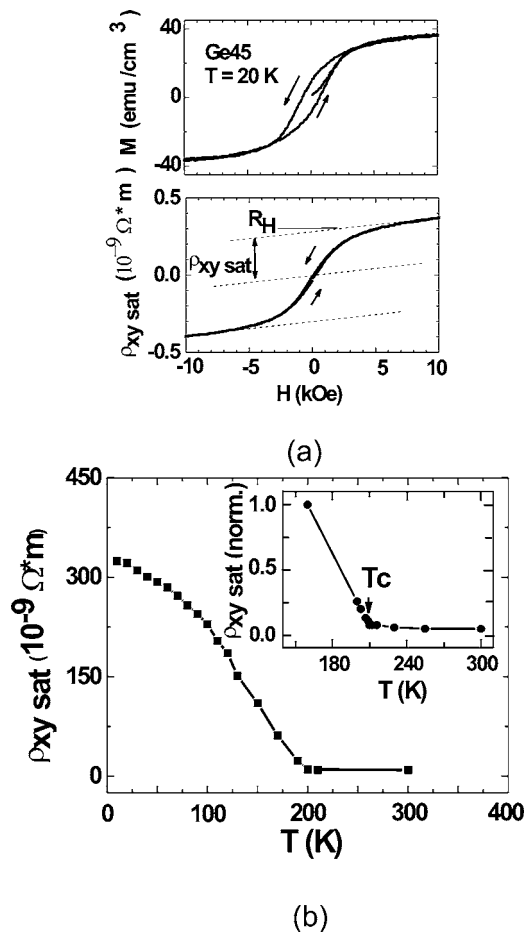


FIG. 3. (a) Comparison of spontaneous magnetization M and anomalous Hall resistivity ρ_{xy} hysteresis curves for Ge45. In the lower panel the construction, which is used to define the ordinary Hall coefficient R_H and the anomalous Hall resistivity at saturation $\rho_{xy\text{sat}}$, is demonstrated. (b) The dependence of the AHE on temperature for Ge45 sample as measured from the saturation anomalous Hall resistivity $\rho_{xy\text{sat}}$ for unpatterned Ge45. The inset shows precise dependence of $\rho_{xy\text{sat}}(\text{norm}) = \rho_{xy\text{sat}}(T)/\rho_{xy\text{sat}}(160 \text{ K})$ on temperature T with $T_c = 209 \text{ K}$ for patterned Ge45.

formation of a similar DMS phase for Ge60 and Ge45.

The high content of magnetic dopants and low mobility of holes with weak dependence on temperature in our insulating Ge(Mn,Fe) films suggest the indirect ferromagnetic exchange involving Mn and Fe ions and mediated by localized holes with formation of BMP (Refs. 8 and 11) as a possible mechanism for stabilization of ferromagnetic ordering in favor of a weaker Ruderman-Kittel-Kasuya-Yoshida (RKKY)-type exchange,¹² which involves delocalized carriers. We connect the positive role of iron as codopant with increased total concentrations of magnetic ions involved in FM exchange, still conserving crystalline ordering. The

magnetic phase transition near 120 K for Ge45 could be connected with percolation of BMP already formed at $T \sim 205 \text{ K}$. Additional experiments aimed to distinguish the BMP mechanism⁸ from ferromagnetic double exchange^{13,14} as another possible mechanism of ferromagnetic ordering are highly desired.

We note that a nonequilibrium diffusion of elements during sequential deposition can result in a stronger localization of carriers in our structures in comparison with ordinary codeposition procedure. Actually, theoretical considerations for related layered Ge/Mn structures confirm that increased local concentrations of magnetic ions are energetically favorable, thus promising their higher T_c compared to the uniformly doped structures.¹⁵

In conclusion, we found the carrier-mediated ferromagnetism in inhomogeneous Ge(Mn,Fe) magnetic semiconductor films with $T_c = 209 \text{ K}$, which shows strong AHE and correlation between magnetic and Hall transport properties. We relate the C1FM in our insulating Ge(Mn,Fe) to the indirect exchange between magnetic ions mediated by localized holes. The presented deposition procedure conserves crystalline ordering for high local concentrations of magnetic ions, thus providing increased Curie temperatures.

The authors wish to thank colleagues from the Research Centre Jülich, C. M. Schneider for support and D. E. Bürgler and H. Braak for stimulating discussions.

- ¹Y. D. Park, A. T. Hanbicki, S. C. Erwin, C. S. Hellberg, J. M. Sullivan, J. E. Mattson, A. Wilson, T. F. Ambrose, G. Spanos, and B. T. Jonker, *Science* **295**, 651 (2002).
- ²F. Tsui, L. He, L. Ma, A. Tkachuk, Y. S. Chu, K. Nakajima, and T. Chikyow, *Phys. Rev. Lett.* **91**, 177203 (2003).
- ³Y. D. Park, A. Wilson, A. T. Hanbicki, J. E. Mattson, T. Ambrose, G. Spanos, and B. T. Jonker, *Appl. Phys. Lett.* **78**, 2739 (2001).
- ⁴S. Cho, S. Choi, S. C. Hong, Y. Kim, J. B. Ketterson, Y. C. Kim, and J.-H. Jung, *Phys. Rev. B* **66**, 033303 (2002).
- ⁵S. Choi, S. C. Hong, S. Cho, Y. Kim, J. B. Ketterson, C.-L. Jung, K. Rhie, B.-J. Kim, and Y. C. Kim, *J. Appl. Phys.* **93**, 7670 (2003).
- ⁶H. Braak, R. R. Gareev, D. E. Bürgler, P. Grünberg, R. Schreiber, and C. M. Schneider, *J. Magn. Magn. Mater.* **286**, 46 (2005).
- ⁷A. P. Li, J. Shen, J. R. Thompson, and H. H. Weitering, *Appl. Phys. Lett.* **86**, 152507 (2005).
- ⁸A. Kaminski and S. das Sarma, *Phys. Rev. Lett.* **88**, 247202 (2002); *Phys. Rev. B* **68**, 235210 (2003); **70**, 115216 (2004).
- ⁹H. Ohno, *Science* **281**, 951 (1998).
- ¹⁰C. Zeng, S. C. Erwin, L. C. Feldman, A. P. Li, Y. Song, J. R. Thompson, and H. H. Weitering, *Appl. Phys. Lett.* **83**, 5002 (2003).
- ¹¹E. L. Nagaev, *Phys. Rep.* **346**, 387 (2001).
- ¹²T. Dietl, H. Ohno, F. Matsukura, J. Cibert, and D. Ferrand, *Science* **287**, 1019 (2000).
- ¹³H. Akai, *Phys. Rev. Lett.* **81**, 3002 (1998).
- ¹⁴P. Kacman, *Semicond. Sci. Technol.* **16**, R25 (2001).
- ¹⁵A. Continenza, F. Antonella, and S. Picozzi, *Phys. Rev. B* **70**, 035310 (2004).